Excess Conductivity and Critical Physical Parameters of Y Substituted Ca Site of Bi: 2223 High T_c Superconductors

Abstract

We presented here the fluctuation induced excess conductivity in $Bi_{1.7}Pb_{0.3}Sr_2Ca_{2-x}Y_xCu_3Oy$ superconductors with various x values ($0.00 \leq x \leq 0.50$). The logarithmic plots of excess conductivity ($\Delta\sigma$) and reduced temperature (ε) reveal three different values of the order parameter dimensional exponents against a decrease of temperature corresponding to two different values of crossover temperatures. In the critical field region, the order parameter exponents are two dimensional (2D) as x increases up to 0.20, but it is changed to three dimensional (3D) with further increase of x up to 0.50. While, the order parameter exponents are not systematic with Y in both normal and mean field regions, and they are fluctuated between zero dimensional /short wave (0D/SW), qusi-2D, qusi-1D and 3D. On the other hand, the coherence lengths, inter-plane spacing, interlayer coupling, Ginsburg number and anisotropy are calculated and their values are generally increased by increasing x up to 0.50, whears G-L parameter, critical magnetic fields and critical current density are decreased. The possible reasons for the above findings are also mentioned.

Keywords: Fluctuation; Excess conductivity; Critical parameters, Order Parameter and Critical Fields

Introduction

The doping processes in high temperature superconductors have been used early to improve their properties in parallel with special focusing on their applications [1,2]. The Bi: 2223 superconducting system with T_C of 110 K is the most widely studied superconductor, because it is differ with the other superconductors in the number of both CuO_2 planes and Ca layers [3]. Furthermore, the Bi: 2223 system has higher critical current density J_c and critical magnetic fields H_c as compared to Y: 123 systems [4,5].

The well established diagram of the high temperature superconductors against carrier concentration indicate that the systems are Mott-Hubbard insulator in the under doped region and superconductor in the intermediate range, whears in the over doped region they are normal metal [6-7]. However, carrier concentration in the high T_c superconducting systems may be varied either by varying the doping content or oxygen deficient, leading to dramatic changes in the transport behavior, and simultaneously influence the T_c values [8,9].

Due to short coherence length and high T_c in superconductors, the thermal fluctuation of superconducting order parameter has been early observed as excess conductivity [10-11]. The fluctuation of Cooper pairs begin to be created spontaneously at a temperature higher than twice mean field temperature T_c^{mf} ($T \geq 2T_c^{mf}$), and normally increases as the temperature approaches critical temperature T_c. The mean field temperature T_c^{mf} is the temperature at which the fluctuation induced conductivity regime separates from the critical fluctuation regime, and normally obtained close to T_c [12-15]. This is simply obtained from the optimum value of the ($d\rho/dT$) against temperature plot as a simple method.

The fluctuation induced conductivity (FIC) analyses reveal that the contribution of excess conductivity is mainly due to Gaussian and critical fluctuations in the mean field and critical field regions, respectively [16]. Gaussian fluctuation is probably dominant in the temperature region above the T_c^{mf} when the fluctuation in the order parameter is small and the interactions between Cooper pairs can be neglected. While the critical fluctuation occurs in the critical field region below the T_c^{mf} when the fluctuations in the order parameter are large and the interactions between Cooper pairs is considered.

The variation of induced excess conductivity due to Gaussian fluctuation with the reduced temperature ϵ helps for finding the dimensional exponents, coherence lengths, interlayer coupling, inter-plane spacing and crossover temperatures [17-18]. The dimensional exponents in high T_c materials are found to be zero dimensional or spin wave (0D/SW), one dimensional

(1D), two dimensional (2D) and three dimensional (3D). It is seen that the dimensional crossover takes place between any two different dimensions regions, and it is mainly obtained above T_c in most of high T_c systems [19-20].

The fluctuation conductivity is an important topic because it is directly examines the possibility for the electron pairs formation at a temperature above T_c. According to the one of existing concept, the pseudogap is formed above T_c due to superconducting fluctuations, and usually leads to electron pairs formation, which serves as a precursor to the transition into superconducting state. Nevertheless the fluctuation studies based on pure Bi:2223 superconducting systems in the vicinity of T_c are well described by 2D or qusi-2D nature as a result of good interlayer coupling. It may also become 3D depending on a heat treatment that modifies the state of microscopic disorder and induces spatial fluctuations near T_c [21]. The doping of rare earth elements at Ca sites in Bi:2223 superconductors mutually have different results based on fluctuation study of induced excess conductivity which may be alters the carrier concentration in the CuO_2 planes. The doping of Pr, Ce, Gd and Cd doped at Ca sites in Bi:2223 system suggest 2D superconducting order parameter, and a distinct 2D-3D crossover behavior is obtained near T_c [22-27]. Furthermore, the doping at sufficiently high dopant concentrations leads to a T_c depression and usually causes a metal-insulator transition. But these studies however, do not discuss in details the effects of Y substitution in Bi:2223 systems on the behavior of superconducting fluctuation especially in the over doped region. Moreover, some of the physical parameters such as coherence lengths, inter-plane spacing, interlayer coupling, G-L parameter, anisotropy, critical fields and critical current are not summarized in details. However, structural and superconducting properties of $Bi_{1.7}Pb_{0.3}Sr_2Ca_{2-x}Y_xCu_3Oy$ superconductors with various x values are well investigated by A. Sedky [28]. Although T_c was gradually decreased by increasing x up to 0.50, it found that Y has a higher solubility in the Bi (Pb):2223 system and is less detrimental to the superconductivity as compared with the other rare earth elements R. At present, there is an ample interest for investigating the fluctuation induced conductivity of the same bath of samples and able to calculate some of superconducting physical parameters.

Experimental Results and Discussion

As reported by A.Sedky [28], $Bi_{1.7}Pb_{0.3}Sr_2Ca_{2-x}$ Y_xCu3O_y samples are prepared by using solid-state reaction method and tested for phase purity by XRD. The results of XRD patterns indicated that most of high intensity peaks belong to the 2223 tetragonal phase with a few low intensity peaks belong to 2212 phase. The c-parameter is decreased with increasing x,

whereas a-parameter increases. The decrease in c- parameter with Y content is due to smaller ionic size of Y^{3+}(1.02 Å) ions compared to the Ca^{2+} (1.12 Å) at the same 8-fold coordination. While, the increase in the a-parameter may result from a decrease in the hole carrier concentration per Cu ion, which weakens the Cu-O bond.

The electrical resistivity of the samples $\rho = \frac{RA}{\ell}$ are obtained as a function of temperature using the standard four-probe technique in closed cycle refrigerator [cryomech compressor package with cryostat Model 810-1812212, USA] within the range of (10-300K). Nanovoltameter Keithley 2182, current source Keithley 6220 and temperature controller 9700 (0.001 K resolution) are used in this experiment. Silver paste is used for making currents and voltage contacts. A current (1-5) mA is passing through the sample and the voltage across the sample is measured by using nanovoltameter. The values of resistivity are obtained from the values of voltage and sample dimensions A and ℓ. The gradual depression of T_c (ρ = 0.00) from 106 K to 101, 93, 79, 55 and 21 K by Y^{3+} substitution from up to 0.50 at Ca^{2+} sites is listed in Table 1 and shown in Figure 2(b). This is due to increasing the hole carriers concentration per Cu ion in the superconducting state from the optimum doped region to the over doped region as x increases. In this case, more positive charges are transferred to the Cu-O_2 planes in the Bi:2223 system and helps for decreasing T_c [28-29].

The excess conductivity Δσ due to thermal fluctuation is defined by the deviation of the measured conductivity of σ_m (T) from the normal conductivity σ_n (T) as follows;

$$\Delta\sigma = \left(\frac{1}{\rho_m} - \frac{1}{\rho_n}\right) = \sigma_m - \sigma_n \qquad (1)$$

where ρ_m and ρ_n are the measured and normal resistivity, respectively. ρ_n is obtained from the measured resistivity ρ_m at $T \geq 2T_c$ by applying the least square method to the Anderson and Zou relation , $\rho_n(T) = A + BT$ [30]. ρ_n(T) is calculated in terms of A and B parameters that obtained from the linear fit of the measured resistivity ρ_m(T) as shown in Figure 1(a-f).

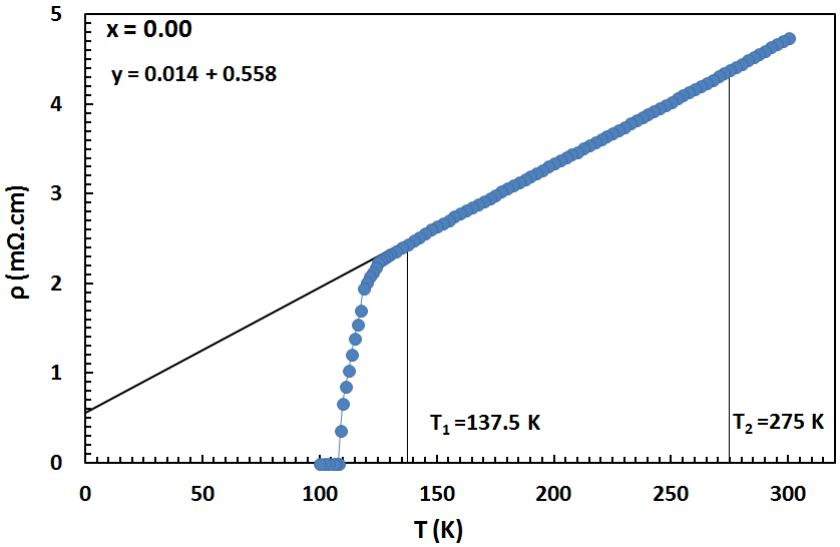

Figure 1 (a): Resistivity versus temperature for Y doped Bi:2223 samples (x= 0.00)

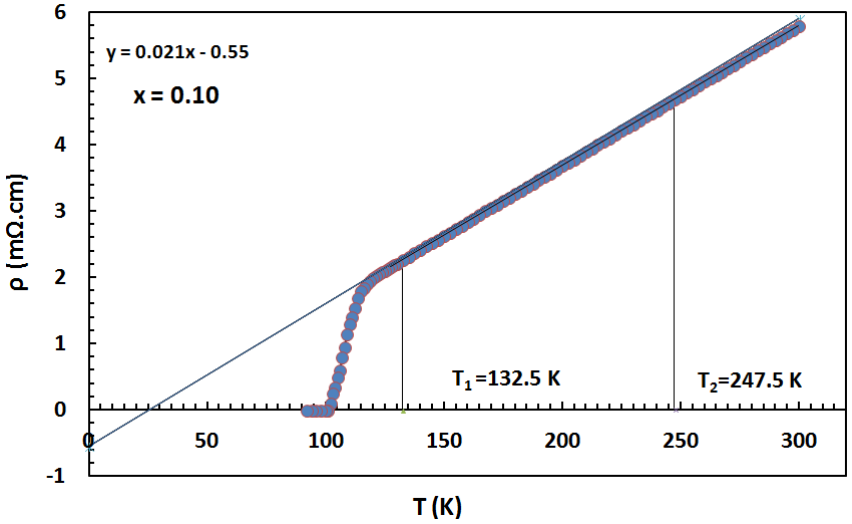

Figure 1 (b): Resistivity versus temperature for Y doped Bi:2223 samples (x=0.10)

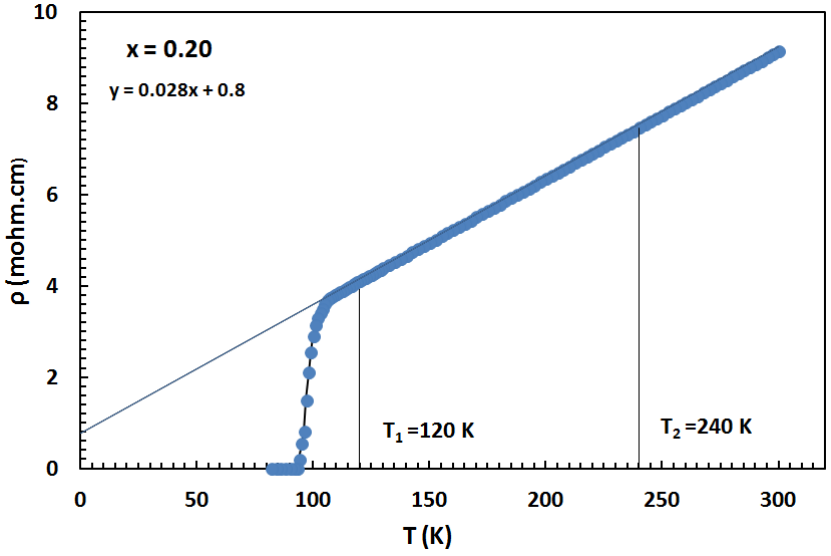

Figure 1 (c): Resistivity versus temperature for Y doped Bi:2223 samples (x=0.20)

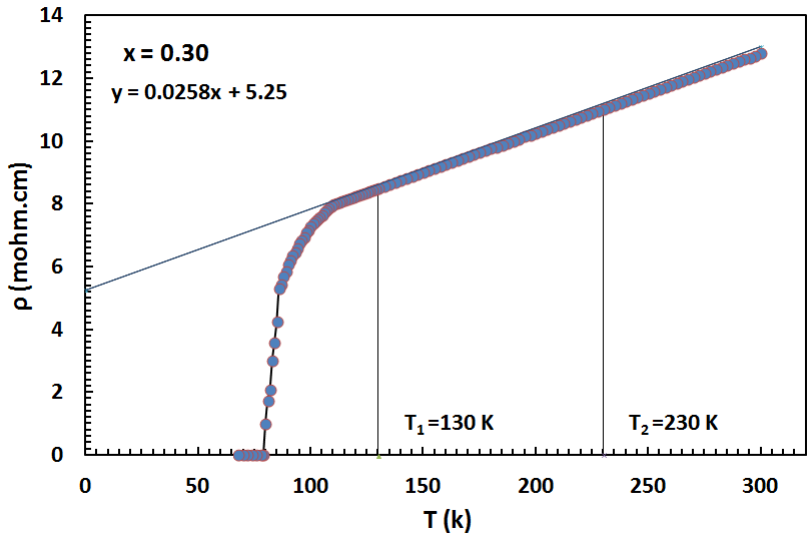

Figure 1 (d): Resistivity versus temperature for Y doped Bi:2223 samples (x=0.30)

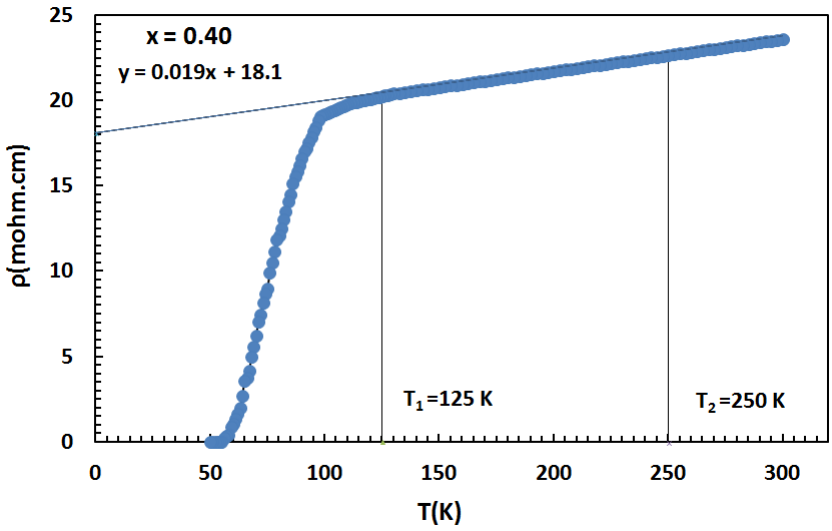

Figure 1 (e): Resistivity versus temperature for Y doped Bi:2223 samples (x=0.40)

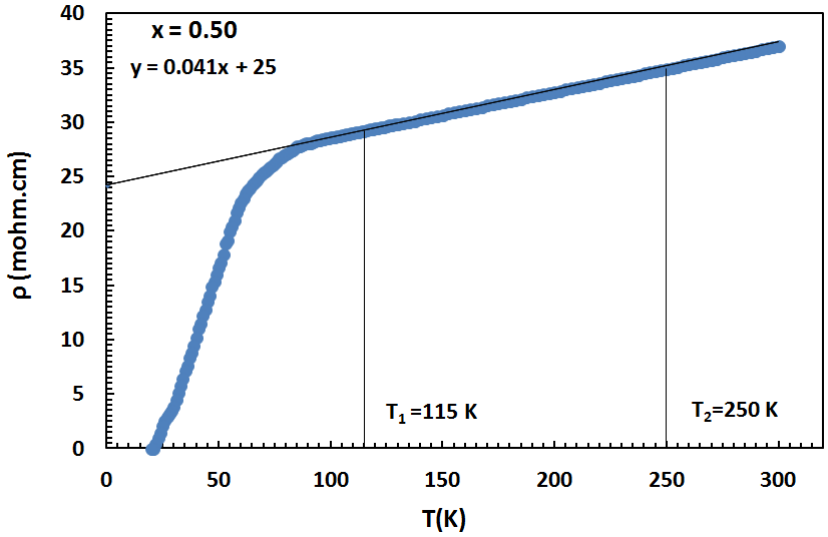

Figure 1 (f): Resistivity versus temperature for Y doped Bi:2223 samples (x =0.50)

In order to estimate the paraconductivity, Aslamazov and Larkin (AL) deduced the following relation for the fluctuation- induced excess conductivity Δσ as [30];

$$\Delta\sigma = A\varepsilon^{-\lambda} \qquad (2)$$

Here, $A = \frac{e^2}{32\hbar\xi_c(0)}$ for 3D, $A = \frac{e^2}{32\hbar d}$ for 2D and $A = \frac{e^2\xi_c(0)}{32\hbar S}$ for 1D, e is the electronic charge, d is the interlayer spacing between two successive CuO_2 planes, ħ is the reduced Planks' constant, ξ_c (0) is the c-axis 3D coherence length at zero temperature, S is the wire cross-sectional area of the 1D system, λ is an exponent related with the actual conduction dimensionality. The values of the exponent's λ are 2, 0.5, 1 and 1.5 for (0D/SW), 3D, 2D and 1D fluctuations respectively, and ε is the reduced temperature given by $\varepsilon = \frac{T - T_c^{mf}}{T_c^{mf}}$ [30-32].

Where T_c^{mf} is the mean field temperature above it the interactions between Cooper pairs can be neglected. T_c^{mf} for all samples are estimated from the peak of dρ/dT against temperature plot as shown in Figure 2 (a), and similar values are listed in Table 1. However, the variation of T_c and T_c^{mf} against x content is shown in Figure 2 (b). It is clear that T_c^{mf} is decreased as x increases as well as T_c.

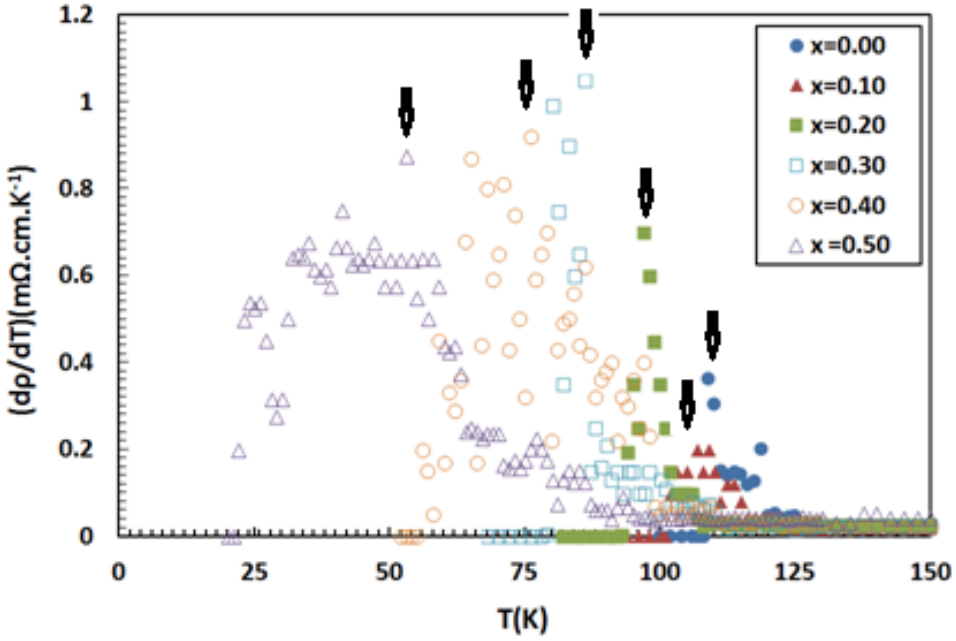

Figure 2 (a): dρ/dT versus temperature for Y doped Bi:2223 samples

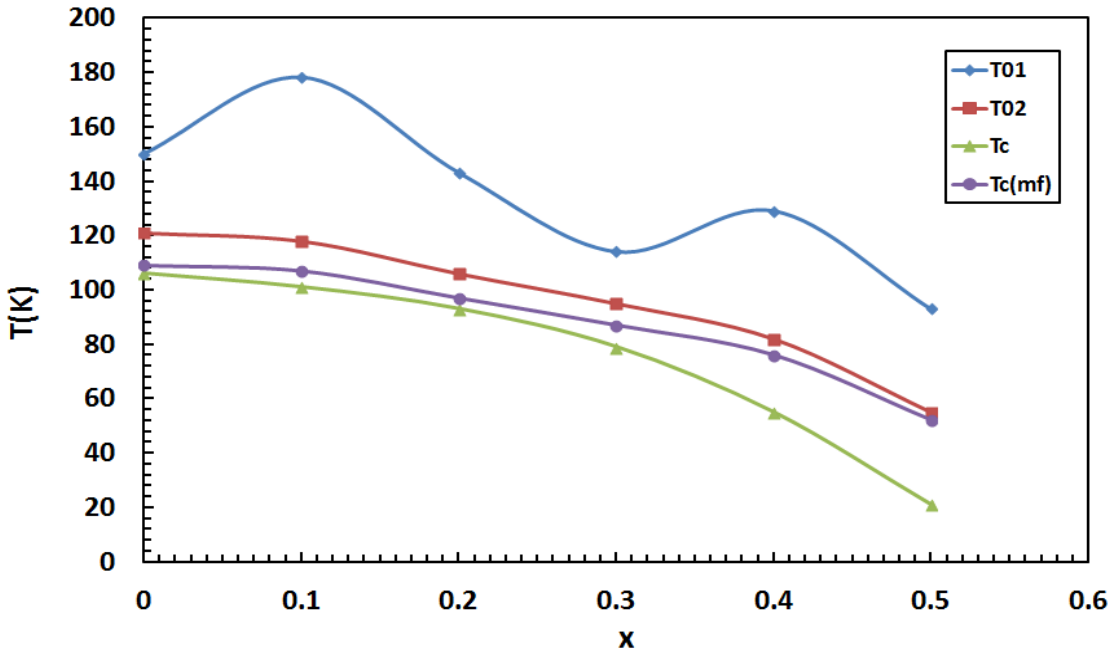

Figure 2(b): T_c, T_c^{mf} and T_o versus x for Y doped Bi:2223 samples

We have calculated and plotted the excess conductivity lnΔσ against reduced temperature lnε and shown in Fig. 3(a-f). However, it is evident from the fitting that there are two distinct changes in the slope of each plot; the first is in the normal field region, while the second is in the mean field region. The corresponding temperatures where the slope change occurs are designated as the crossover temperatures T_{o1} and T_{o2}. The variation of crossover temperatures against x is shown in Figure 2(b), and similar values are listed in Table 1. It is clear that T_0^1 is

not systematic with x content, but it is generally decreased as x increases as compared to pure sample. The higher value of T_0^1 in the normal field region at x = 0.10 means that a sizable fraction of Y may be residing outside the superconducting grains, and helps for shifting the cross-over temperature to higher value. As x increases above 0.10, a convenient fraction of Y is residing inside the grains, and then T_0^1 shifted to lower values [33]. T_{02} is gradually decreased as x increases as well as T_c and T_c^{mf} behaviors.

The crossover behavior could be explained according to the highly anisotropy of superconductor, where the charge carriers move more readily in some directions than in the others. Further, the charge carriers have ability to move along the superconducting planes in the superconductor within a range of temperature selected at which the thermal fluctuations of charge carriers exist. A crossover behavior due thermal fluctuations takes place by cooling the superconductor down to a lower temperature, and therefore the charge carriers may move between the superconducting planes and crossover from one plane to another. This means that the charge carriers tend to move more freely in the whole sample before they make pairs in the mean field region above T_c[34-36].

Table 1: T_c , T_c^{mf}, T_0 , *J*, d, $\xi_c(0)$, λ_I , λ_{II} and λ_{III} for Y doped Bi:2223 samples

x	T_c K	T_c^{mf} K	T_{01} K	T_{02} K	*J*	d (Å)	$\xi_c(0)$ (Å)	d/ $\xi_c(0)$	λ_I	λ_{II}	λ_{III}
0.00	106	109	150	121	0.59	21.30	8.18	2.61	0.59 **(qusi-2D)**	2.37 **(0D/SW)**	0.91 **2D**
0.10	101	107	178	118	0.6	24.51	9.49	2.58	1.34 **(qusi-1D)**	0.49 **3D**	1.09 **2D**
0.20	93	97	143	106	0.6	40.80	15.80	2.58	0.9 **2D**	0.34 **3D**	1.17 **2D**
0.30	79	87	114	95	0.61	49.83	19.46	2.56	0.81 **2D**	2.56 **(0D/SW)**	0.45 **3D**
0.40	55	76	129	82	0.62	60.35	23.76	2.54	0.15 **(qusi-3D)**	2.52 **(0D/SW)**	0.46 **3D**
0.50	21	52	93	55	0.64	75.53	30.21	2.50	0.65 **(qusi-2D)**	1.97 **(0D/SW)**	0.34 **3D**

Three different exponents of the order parameter dimensionality could be obtained from the slopes of each plot as shown in Figure 3 (a-f). These values are arranged towards low temperature region as λ_I , λ_{II} and λ_{III} for x = 0.00, 0.10, 0.20, 0.30, 0.40 and 0.50, respectively. The first exponents λ_I are obtained in the normal field region at a temperature range of ln ε ($0.00 \geq \ln \varepsilon \geq 1.5$), and their values are 0.59 (qusi-2D), 1.34 (qusi-1D), 0.90

(2D), 0.81 (2D), 0.15 (qusi-3D) and 0.65 (qusi-2D). The second exponents λ_{II} are obtained at the mean field region at a temperature range of ln ε (-0.50 ≥ ln ε ≥ -2.5), and their values are 2.37 (0D/SW), 0.49 (3D), 0.34 (3D), 2.56 (0D/SW), 2.52 (0D/SW) and 1.97 (0D/SW). The third exponents λ_{III} are obtained in the mean field region at a temperature range of ln ε (-2 ≥ ln ε ≥ -4.5) and their values are 0.91 (2D), 1.09 (2D), 1.17 (2D), 0.45 (3D), 0.46 (3D) and 0.34 (3D). The appearance (0D/SW) in these types of samples may be due to short wave length fluctuations in the considered region [26, 27]. Our interesting point here is observed for the third values of exponents in the mean field region, where the order parameter is shifted from 2D to 3D as the x increases above 0.20. This is may be related to the effective length in the direction perpendicular to the current flow which is found to be more reduced in Y doped Bi:2223 as x increases up to 0.50 [37]. Further, the obtained (0D/SW) of the order parameter below T_c is due critical fluctuations in the conductivity region of microscopic granular superconductor, and it is extremely sensible to applied magnetic field [21].

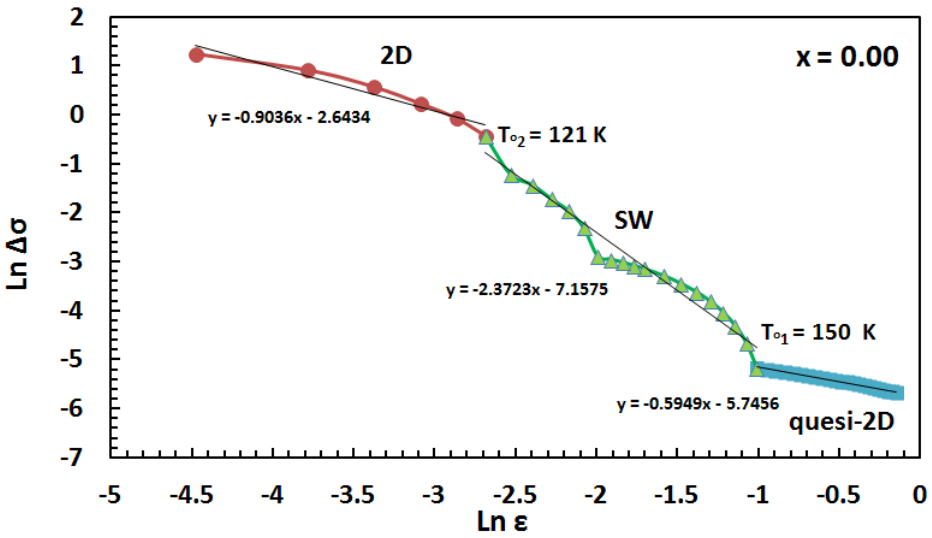

Figure 3(a): lnΔσ against lnε for Y doped Bi:2223 samples (x = 0.00)

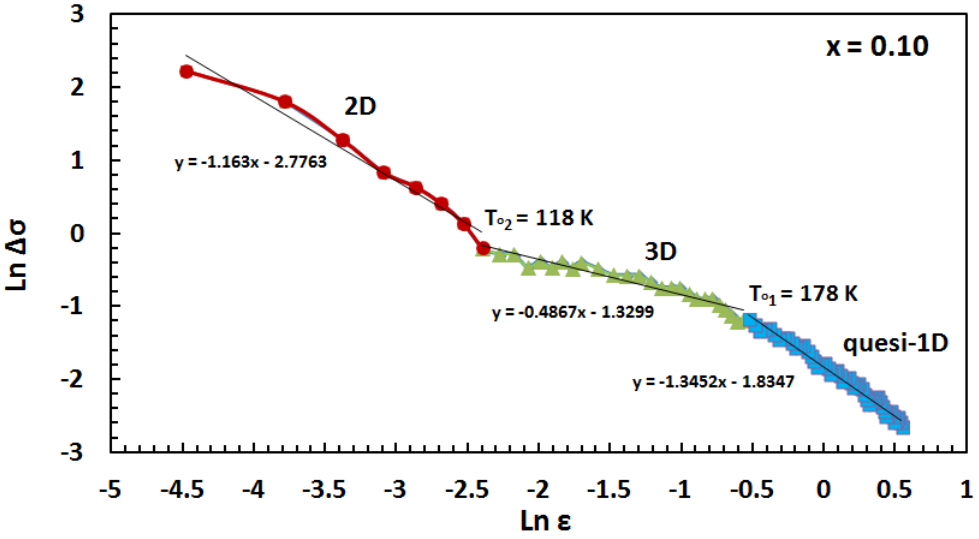

Figure 3(b): lnΔσ against lnε for Y doped Bi:2223 samples (x = 0.10)

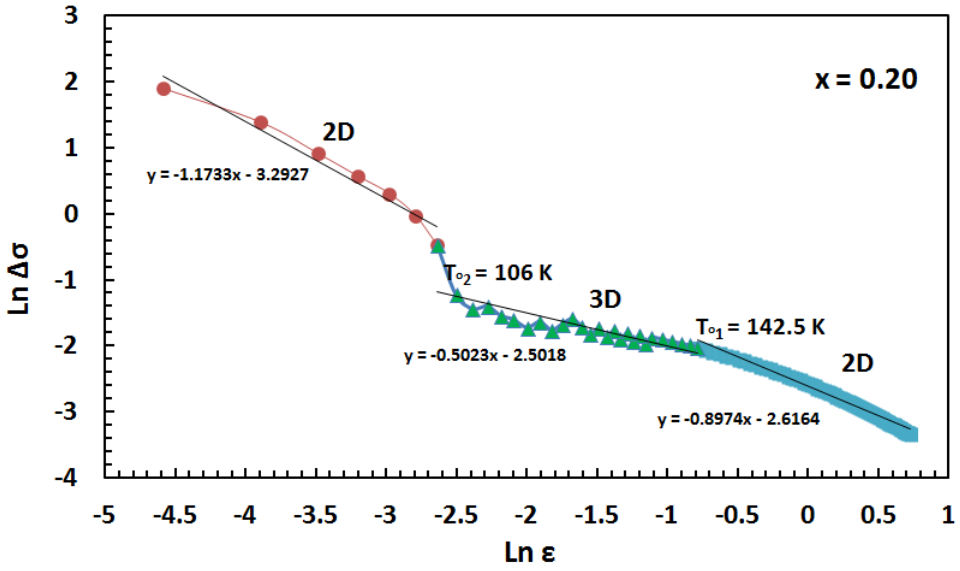

Figure 3(c): lnΔσ against lnε for Y doped Bi:2223 samples (x = 0.20)

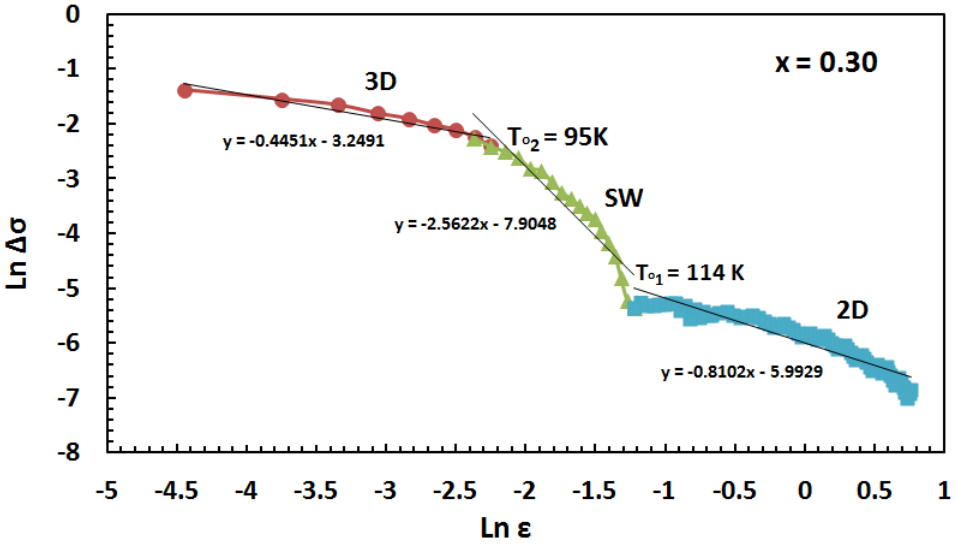

Figure 3(d): lnΔσ against lnε for Y doped Bi:2223 samples (x = 0.30)

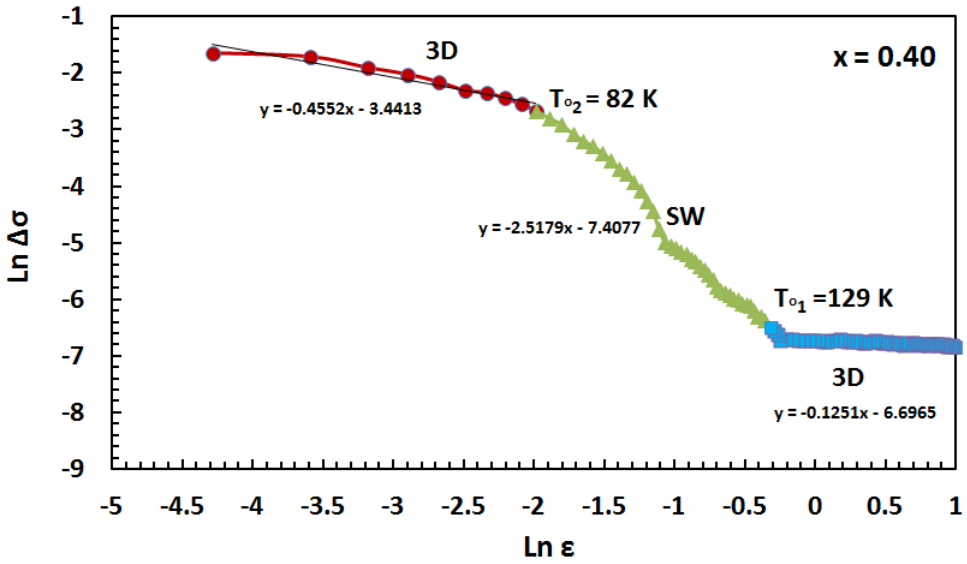

Figure 3(e): lnΔσ against lnε for Y doped Bi:2223 samples (x = 0.40)

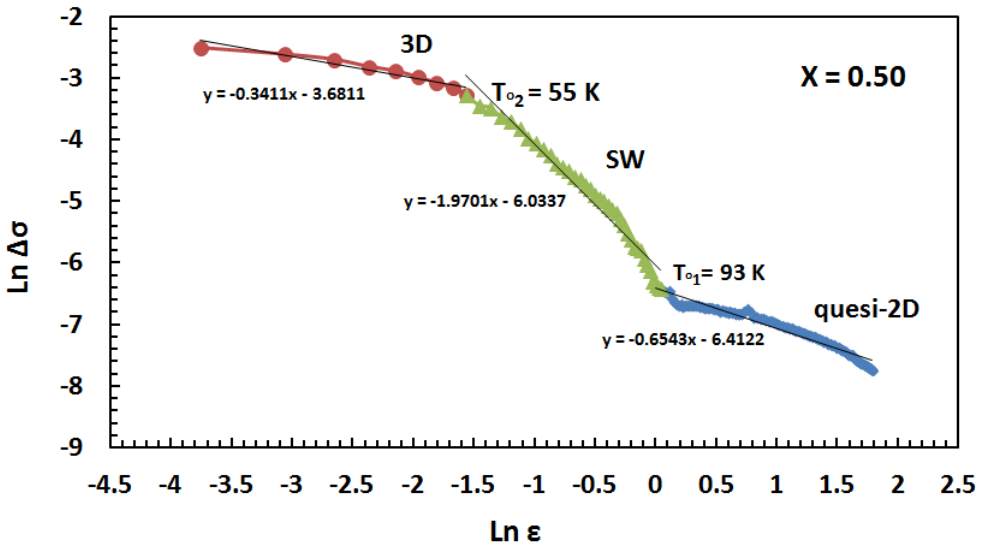

Figure 3(f): lnΔσ against lnε for Y doped Bi:2223 samples (x = 0.50)

Anyhow, the crossover behavior occurs at a temperature T_0 is given by [38,39];

$$T_0 = T_c^{mf} \exp\left(\frac{2\xi_c(0)}{d}\right)^2 \qquad (3)$$

, where $\xi_c(0)$ is given by $\xi_c(0) = \frac{dJ^{\frac{1}{2}}}{2}$ and J is the interlayer coupling expressed by $J = \ln\frac{T_0}{2T_c^{mf}}$ [40,41]. The average values of interlayer coupling J are calculated in terms of the values of T_{o2} and T_c^{mf}, and listed in Table 1. It is found that J slightly increased by increasing x, and their values are between 0.59 and 0.64 for all samples. The samples of x =

0.00, 0.10 and 0.20 are 2D nature, and the intersect $A = \frac{e^2}{32\hbar d}$ for 2D. Therefore, d and $\xi_c(0)$ are calculated from the values of A and *J*, respectively. While the samples of x = 0.30, 0.40 and 0.50 are 3D nature, and the intersect $A = \frac{e^2}{32\hbar \xi_c(0)}$. for 3D. Therefore, $\xi_c(0)$ and d are calculated from the values of A and J, respectively.

Figure 4 shows the behavior of both d and $\xi_c(0)$ against x, and similar values are listed in Table 2. It is clear that both d and $\xi_c(0)$ are increased as x increases, but the values of d are higher than that of $\xi_c(0)$, indicating the 2D nature of superconductivity, in agreement with the reported data [21-27]. The increase of ξ_c (0) at (x > 0.20) indicates that Y substitution shifts the hole carriers from the optimum doped region of the pure sample towards the over doped region [42]. Similar results are obtained by Wen et al. [28] for La: 214 superconductors. They found a drop of the coherence length in the under-doped region followed by an increase in the over-doped beside an increase of hole-concentration. The values of [d/ξ_c (0)] shown in Table 1 are between 2.51 and 2.60 for all samples, which is probably related to a constant values of *J* as discussed above.

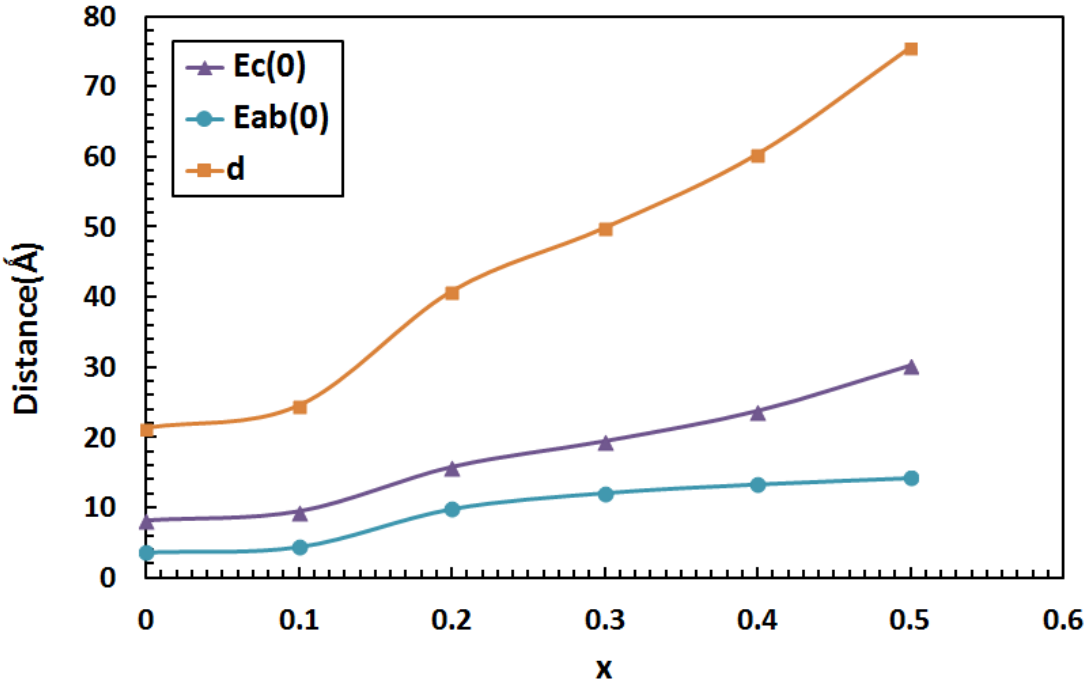

Figure (4): d , $\xi_{ab}(0)$ and $\xi_c(0)$ versus x for Bi:2223 samples

The critical field H_c (0), lower critical field $H_{c1}(0)$, upper critical fields $H_{c2}(0)$ and critical current density at 0 K are estimated by the following relations [42, 44-46]

$$H_c(0) = \frac{\phi_0}{2\sqrt{2}\pi\lambda(0)\xi_c(0)}; \qquad H_{c1}(0) = \frac{H_c(0)\ln\kappa}{\sqrt{2}\kappa} \tag{4a}$$

$$H_{c2}(0) = \sqrt{2}\kappa H_c(0); \qquad J_c(0) = \frac{4\kappa H_{c1}(0)}{3\sqrt{3}\lambda(0)\ln\kappa} \tag{4b}$$

$\phi_0 = 2.07\times10^{-15}(T.m^2)$, κ is Ginsberg-Landau parameter of the superconducting system given by; $\kappa = \frac{\lambda(0)}{\xi(0)}$, where λ(0) is the London penetration depth at 0 K, which is about 300 nm for Bi:2223 superconductors [47]. However, the values of κ listed in Table 2 are decreased as x increases up to 0.50. Similar behavior is obtained for the critical values of fields and current as shown as in Figures 5 (a,b). This behavior may be due to a decrease of grain boundaries resistance and superconducting volume fraction of (Bi, Pb)-2223 single phase as x increases [42, 47].

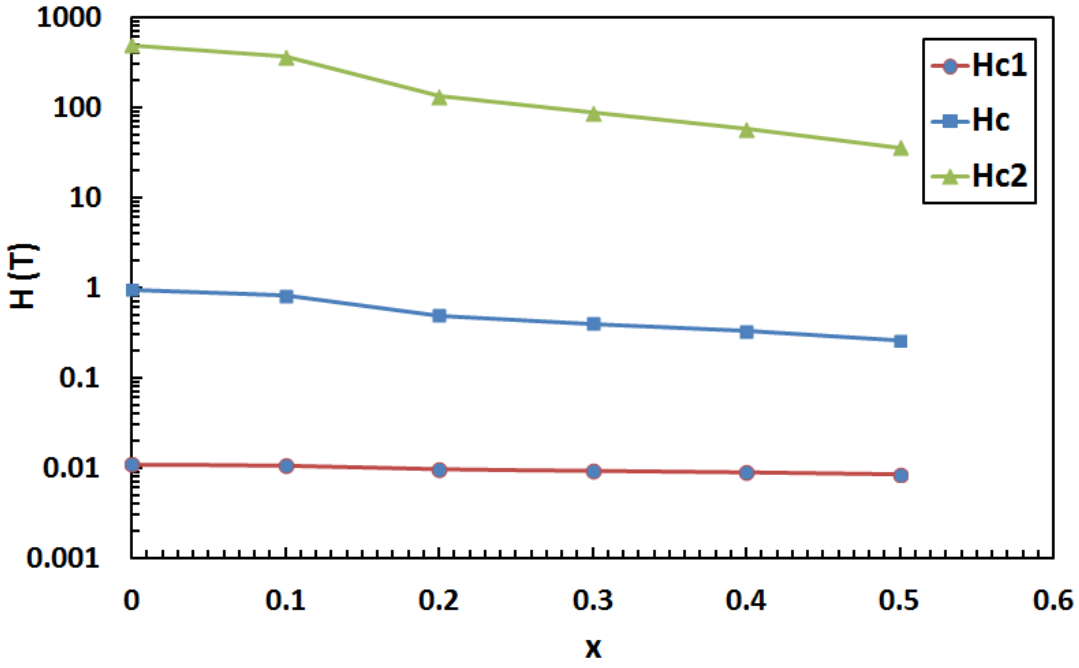

Figure 5(a) : Critical magnetic fields versus x for Bi:2223 samples

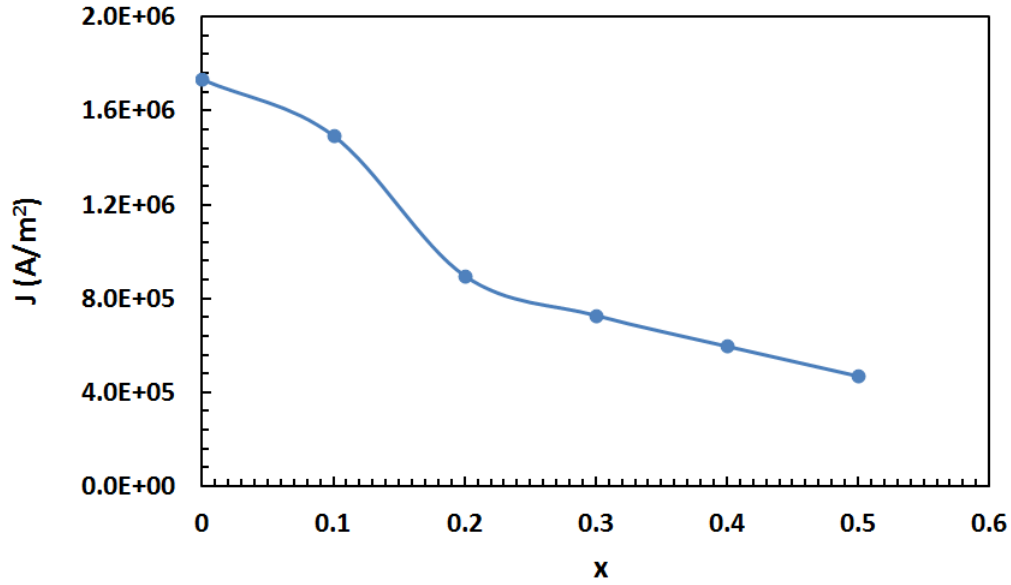

Figure 5(b) : Critical current density versus x for Bi:2223 samples

The anisotropy parameter could be obtained using the relation [48];

$$\gamma = [\frac{0.71K_B}{\sqrt{N_G}B_c^2(0)\xi_c^3(0)}]^{\frac{1}{2}} \qquad (5)$$

K_B is Boltzmann constant and N_G is Ginzberg reduced number given by the relation; $N_G = \frac{T_0 - T_c}{T_c}$. From the values of anisotropy, the in-plane coherence length at 0 K, $\xi_{ab}(0)$ could be obtained using the relation, $\gamma = \frac{\xi_{ab}(0)}{\xi_c(0)}$. It is clear from Table 2 that both N_G , γ and ξ_{ab} are increased as x increases up to 0.50. Similar behavior between the above parameter and x are also obtained in Figures 4 and 6.

Table 2: H_c , H_{c1}, H_{c2}, $J_c(0)$, Gi , NG , γ and $\xi_{ab}(0)$ for Y doped Bi:2223 samples

x	*K*	H_c (T)	H_{c1} (T)	H_{c2} (T)	J_c (A/m^2)	Gi	N_G	γ	ξ_{ab} (Å)
0.00	366.748	0.95	0.0109	490.94	17.3×10^5	5.48×10^{-3}	0.14	0.44	3.60
0.10	316.122	0.82	0.0106	364.76	14.9×10^5	3.70×10^{-3}	0.17	0.46	4.37
0.20	189.873	0.49	0.0096	131.59	8.97×10^5	1.13×10^{-3}	0.14	0.62	9.80
0.30	154.162	0.40	0.0093	86.75	7.28×10^5	0.54×10^{-3}	0.20	0.62	12.07
0.40	126.263	0.33	0.0089	58.19	5.96×10^5	0.18×10^{-3}	0.49	0.56	13.31
0.50	99.3049	0.26	0.0085	35.99	4.69×10^5	0.016×10^{-3}	1.60	0.47	14.20

The Ginzburg number, Gi, defines the order thermal fluctuations in a superconductor is given by [49-50];

$$G_i = [\frac{\pi\kappa^2\xi_0(c)K_B T_c \mu_0}{2\phi_0^2}]^2 \qquad (6)$$

, where $\mu_0 = 4\pi\times10^{-7}$ A/m and K_B is Boltzmann constant. The values of Gi are calculated for all samples and shown in Figure 6, and similar values are listed in Table 2. It is found that the values of Gi are decreased from 5.48 $x10^{-3}$ to 0.016 $x10^{-3}$ as x increases up to x = 0.50. These values are comparable with the reported, $G_i = (10^{-3}\text{-}10^{-4})$ for HTSC, and they are several orders of magnitude larger than 10^{-9} for conventional superconductor. [51-52]. Decreasing the values of G_i support the decrease of critical temperature and also the shift of order parameter dimensionality from 2D to 3D as x increases.

However, the fluctuation induced excess conductivity study for the x -doped Bi (Pb):2223 phase are considered by the following points; (i) decreasing the T_c^{mf} as well as T_c ; (ii) appearance of three different exponents corresponding to two crossover temperatures; (iii) In the critical field region, the order parameter exponents are (2D) up to x = 0.20, but it is changed to (3D) up to x = 0.50; (iv) increasing the coherence lengths, inter-plane spacing, interlayer coupling, Ginzberg number and anisotropy; (v) decreasing the G-L parameter, critical magnetic fields and critical current density.

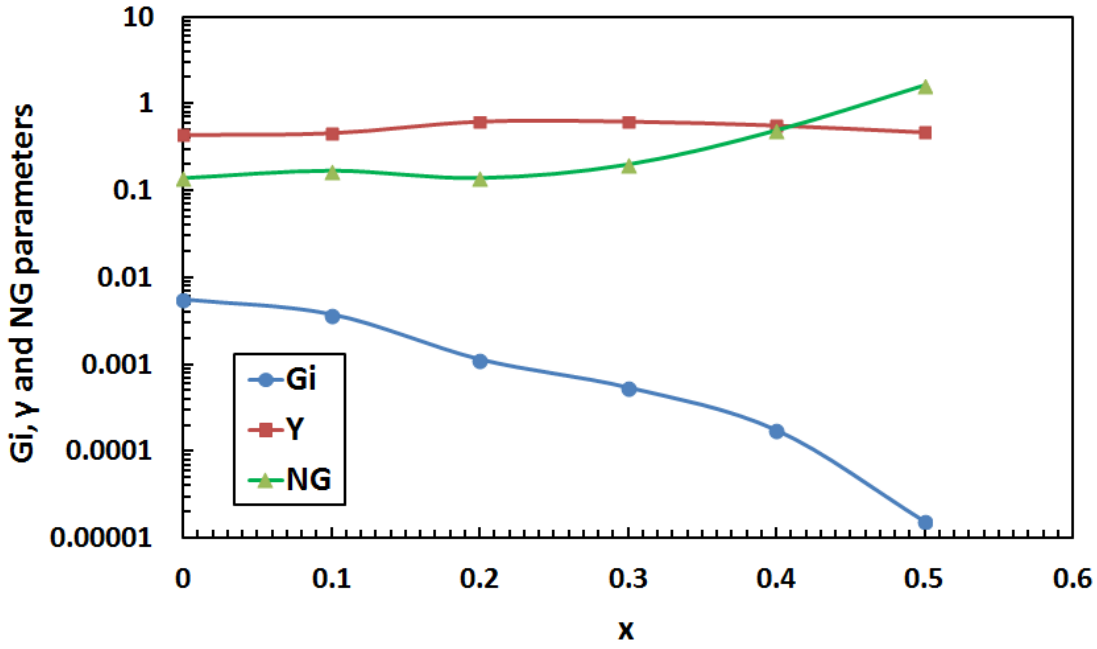

Figure (6) : Gi , γ and N_G versus Y content for Bi:2223 samples

This is due to some reasons such as; decreasing c-lattice parameter by Y substitution at Ca at the same 8-fold co-ordination; increasing the hole carriers concentration per Cu ion in the superconducting state as a result of more positive charges transferred to the Cu-O layer; the excess oxygen arising from the replacement of 2CaO by one Y_2O_3 molecule; increasing both coherence lengths and anisotropy. The consistency of these points gives a fair degree of certainty to appearance the fluctuation induced excess conductivity of Y substitution in Bi (Pb):2223 system.

Conclusion

Fluctuation induced excess conductivity in Y doped Bi: 2223 is reported. We have shown three different values of the order parameter exponents corresponding to two crossover temperatures due to shifting the order parameter dimensionality against a decrease of temperature. In the critical field region, the order parameter exponents are two dimensional (2D) as x increases up to 0.20, but it is changed from 2D to three dimensional (3D) with further increase of x up to 0.50. While, the order parameter exponents are fluctuated between zero dimensional/ short wave fluctuation (0D/SW), qusi-2D, qusi-1D and 3D in the normal and mean field regions. The coherence lengths, inter-plane spacing, interlayer coupling, Ginzberg number and anisotropy are generally increased by increasing x up to 0.50, whears G-L parameter, critical magnetic fields and critical current density are decreased. The possible reasons for the above findings are also mentioned.

References

1- A. Biju, J. Alloys Compd., 431, 49 (2007).
2- A. Sedky A and W. Al-Battat, Physica B 410, 227 (2013).
3- Jr CP. Poole, HA. Farach, RJ. Cheswick, R. Prozorov, Superconductivity, 2nd ed. Amsterdam: Elsevier (2007).
4- C. Terzioglu C, H. Aydin, O. Ozturk, E. Bekiroglu and I. Belenli. Physica B 403, 3354 (2008).
5- IH. Gul, M.A. Rehman, M. Ali, A. Maqsood , Physica C 432, 71(2005).
6- J.B. Torrance, A. Bezinge, A.I. Nazzal, S.S.P. Parkin, Physica C (162–164), 291 (1989).
7- J.B. Torrance, Y. Tokura, A.I. Nazzal, A. Bezinge, T.C. Huang, S.S.P. Parkin, Phys. Rev. Lett. 61, 1127 (1988).
8- P. Mandal, A. Poddar, B. Ghosh, P. Choudhury, Phys. Rev. B 43, 16, 13102 (1991).
9-A.V. Narlikar, C.V. Rao, S.K. Agarwal, Studies of High Temperature Superconductors, Nova, New York, 1, 341 (1989).
10- M.R. Cimberle, C. Ferdeghini, E. Giannini, D. Marre, M. Putti, A. Siri, F. Federici and A.Varlomov, Phys. Rev. B 55, 14745 (1997).
11- Harabor, A., Harabor, N.A., Deletter, M.: J. Optoelectron. Adv. M. 8, 1072 (2006).
12- D. K. Aswal, A. Singh, S. Sen, M. Kaur, C. S. Viswandham, G. L. Goswami and S. K. Gupta, J. Phys. Chem. Solids 63 , 1797 (2002).
13- M. Sahoo and D. Behera , J. Phys. Chem. Solids 74, 950 (2013).
14- A. Esmaeili and H. Sedghi , J. Alloys Compd. 537, 29 (2012).
15- E.M.M. Ibrahim and S.A.Saleh, Supercond. Sci. Technol. 20, 672 (2007).
16- K. Maki and R.S. Thompson, Phys. Rev. B 39, 2767 (1988).
17- F. Vidal, J. A. Veira, J. Maja, J.J. Ponte, F.G. Alvarado, E. Mordan, J. Amador and C. Cascales, Physica C 156, 807 (1988).
18- F. Ben Azzouz, , M. Annabi, M. Zouaoui and M. Ben Salem, Phys. Stat. Sol. (c) 9, 2978 (2006).
19- C. Baraduc, V. Pagnon, A. Buzdin, J. Henry and C. Ayache, Phys. Lett. A 166, 267 (1992).
20- U.K. Mohapatra, R. Biswal, D. Behera and N. Mishra , Supercond. Sci. Technol. 19, 635 (2006).
21- A.R. Jurelo, J.V. Kunzler, J. Schaf and P. Pureur, Phys.Rev.B 56, 22 ,14815 (1997).
[22] F Vidal, J A Veira, J Maza, J J Ponte, F Alvarado, E. Moran, J. Amador, C. Cascales, A .Castro, M. T. Casais and I. Rasines, Physica C156, 807 (1988).
[23] W. Schnelle, E. Braun, H. Broicher, H. Weiss, H. Geus, S. Ruppel, M. Galffy, W. Braunisch, A .Waldorf, F. Seidler and Wohlleben, Physica C161, 123 (1989)
[24] G. Balestrino, A. Nigro and R. Vaglio, Phys. Rev. B39, 12264 (1989)
[25] J. A. Veira and F. Vidal, Phys. Rev. B42, 8743 (1990)
26- S.M. Khalil, J. Low Temp. Phys. 143 (1-2), 31 (2006).
27- D. R. Mishra, Pramana, J. Physics 70, 3, 535 (2008).
28- A. Sedky, J. Phys. and Chemistry of Solids 70, 483, (2009).
29 M.P. Rojas Sarmiento, M.A. Uribe Laverde, E. Vera López, D.A. Landineza, J. Roa-Rojas, Physica B 398, 360 (2007).
30- R.G. Buckley, J.L. Tallon, D.M. Pooke and M.R. Presland, Physica C 165, 391(1990).
31- A. Das and R. Suryanarayanan, J. Physique 15, 623 (1995).

32- L. Reggiani, R. Vaglio and A. A Varlamo, Phys. Rev. B 44, 9541 (1991).
33- W.E. Lawrence, S. Doniach, in Proc. 12th Conf. Low-Temp. Phys., p. 361, Tokyo (1970).
34 - F. Ben Azzouz, M. Zouaoui, M. Annabi and M. Ben Salem, Phys. Stat. Sol. (c) 3, 9, 3048 (2006).
35- C.J. Lobb, Phys. Rev. B 36, 3930 (1987).
36- P.C. Hohenberg and B.I. Halperin, Rev. Mod. Phys. 49, 435 (1977); W. Anderson and Z. Zou, Phys. Rev. Lett. 60,132 (1988).
37- M. Roumié,W. Abdeen, R. Awad, M. Korek, I. Hassan and R. Mawassi, J Low Temp. Phys. 174, 45 (2014).
38- L.G. Aslamazov and A.I. Larkin, Phys. Lett. A 26, 238 (1968).
39- W.E. Lawrence and S. Doniach, Proc. 12Th Int. Conf. Low Temp. Phys. Kyoto (Edited by E. Kanada), Keigaku, Tokyo, 361 (1971).
40- A. K. Gosh, S. K. Bandyopadhyay and A. N. Basu, J. Appl. Phys. 86 , 3247(1999).
41- A.K. Ghosh, S.K. Bandyopadhyay, P.Barat, Pintu Sen and A.N. Basu, Physica C 264, 255 (1996).
42- A.I. Abou-Aly , R. Awad , M. Kamal ·and M. Anas, J Low Temp Phys 163, 184 (2011).
43- H.H. Wen, H.P. Yang, S.L. Li, X.H. Zeng, A.A. Soukiassian, W.D. Si, , Europhys. Lett. 64, 790 (2003).
44- P.C. Poole, A.H. Farach, J.R. Creswick, R. Prozorov, Superconductivity, 2nd edn. (Academic Press, Elsevier, San Diego, 2007).
45- A.I. Abou Aly, I.H. Ibrahim, R. Awad, A. El-Harizy, A. Khalaf, J. Supercond. Nov. Magn. 23(7), 1325 (2010).
46- A.I. Abou-Aly, R. Awad, I.H. Ibrahim, W. Abdeen, Solid State Commun. 140, 281 (2009).
47- A.Sedky, J. Magnetism and Mag. Materials 277, 293 (2004).
48- A. Petrovie, Y. Fasano, R. Lortz, M. Decrouc, M. Potel, R. Chevrel, O. Fischer, Physica C (460-462),702 (2007).
49- J. Jaroszynski, S. C. Riggs, F. Hunte, A. Gurevich, D. C. Larbalestier, G. S. Boebinger, F. F. Balakirev, A. Migliori, Z. A. Ren, W. Lu, J. Yang, X. L. Shen, X. L. Dong, Z. X. Zhao, R. Jin, A. S. Sefat, M. A. McGuire, B. C. Sales, D. K. Christen, and D. Mandrus, Phys. Rev. B 78, 064511 (2008).
50- M. O. Mun, S. I. Lee, and W. C. Lee, Phys. Rev. B 56, 14668 (1997).
51- Z. Pribulova, T. Klein, J. Kacmarcik, C. Marcenat, M. Konczykowski, S. L. Bud'ko, M. Tillman, and P. C. Canfield, Phys. Rev. B 79, 020508 (2009).
52- Kim, S, Choi, C, Jung, M, Yoon, J, Jo, Y, Wang, X, Chen, X, Wang, XL, Lee, S & Choi, K, Journal of Applied Physics 108 (6), 063916 (2010).